Gourlay, T.P., Cook, S. 2004 Flow past a ship radiating a bore in a channel. *Journal of Engineering for the Maritime Environment* 218, Part 1, pp. 31-40.

Flow Past a Ship Radiating a Bore in a Channel

Tim Gourlay[1] & Steven Cook[2]

A theoretical and experimental investigation is made into the phenomenon of ship-radiated bores caused by a vessel travelling in a shallow, narrow channel at a supercritical speed. The very large drag of this flow phenomenon is studied, as well as the conditions under which it occurs. An improved one-dimensional theory is described for predicting the bore properties, and a new theory put forward for predicting flow velocity and free surface height back to the stern of the ship. Results are compared to an experimental investigation of the same phenomenon, for a ship either fixed vertically in its rest position or free to squat.
Keywords: ship, bore, channel, critical speed.

Notation

B	local ship beam
g	acceleration due to gravity
F_h	depth-based Froude number $U / \sqrt{gh}$
F_{lim}	upper Froude number limit of steady subcritical flow
h	still water depth
h_1	bore height above sea floor
L	ship waterline length
LCF	longitudinal centre of floatation
S	ship's displaced cross-section area at any point when stationary
S_{channel}	channel area to undisturbed waterline
S_{disp}	displaced section area to undisturbed waterline
V	bore speed
w	channel width at waterline
W	flow speed behind bore front
x	longitudinal coordinate in the direction of travel
z	local heave (positive upwards)
z_{LCF}	heave at LCF (positive upwards)
β	scaled local free surface height (relative to undisturbed depth) above undisturbed waterline
η	local free surface height above sea floor

[1] Research Fellow, Centre for Marine Science and Technology, Curtin University of Technology, Western Australia (formerly at the Australian Maritime College)
[2] Naval Architect, Brisbane Ship Constructions (formerly at the Australian Maritime College)

1. Introduction

A ship travelling in a channel is observed to periodically radiate solitons ahead of itself, when travelling at close to the "critical speed". This critical speed is the natural speed of long waves in shallow water, given by $\sqrt{gh}$, where g is the acceleration due to gravity and h is the undisturbed water depth. The fact that no steady wave pattern is possible in this region was noted experimentally by Thews and Landweber **[1]**, and extensive theoretical and experimental research has since been conducted into the smooth solitons radiated forward when a ship is travelling at close to the critical speed.

One of the findings of such research is that solitons tend to reach their maximum height and break when the depth-based Froude number $F_h = U/\sqrt{gh}$ (with U the ship speed) reaches between 1.1 and 1.2 **[2,3,4]**. Above this, no smooth solitons can be produced, and a breaking bore is instead radiated ahead of the model. In this case the Korteweg-deVries / Boussinesq type methods cannot be used directly to model the bore, because of energy lost in the breaking bore front. A simple one-dimensional theory and experimental verification were put forward in **[5]** to explain this phenomenon, based on hydraulic jump relations **[6]** and one-dimensional transcritical theory **[7]**.

In this article the preliminary bore theory **[5]** will be improved, based on more accurate nonlinear expressions for the displaced section areas. Also, the method will be combined with steady nonlinear one-dimensional theory **[8]** to predict the flow past the entire ship.

For simplicity we shall concentrate primarily on the case of a ship vertically fixed in its rest position (no squat). However the theory will also be extended to the full problem of a free ship able to squat.

2. Improved one-dimensional bore theory

2.1 Ship vertically fixed in its rest position

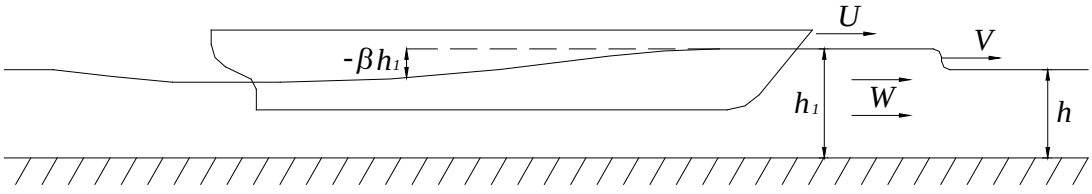

Fig. 1: Bore model and nomenclature

As noted in **[5]**, a developed bore travelling ahead of a ship can be thought of as a hydraulic jump, from still water of depth h ahead of the bore, to a shelf of water of constant depth h_1 and constant flow speed W relative to the still water. The bore front itself is moving at constant speed V relative to the still water. Application of the continuity and force-momentum equations to a control volume straddling the bore front give the hydraulic jump relations **[6]**

$$Vh = (V - W)h_1 \tag{1}$$

$$Wh_1(V - W) = \frac{g}{2}(h_1^2 - h^2) \tag{2}$$

Behind the bore front, and excepting the changed conditions behind the ship, the flow past the ship can be idealized as that of a steady free stream **[5]**. This flow has upstream speed *U*-*W* (where *U* is the ship speed) and undisturbed depth h_1. The minimum possible size of bore which will allow continuity and energy conservation to be satisfied past the ship therefore occurs when the local Froude number behind the bore front is

$$\frac{U - W}{\sqrt{gh_1}} = F_{\lim} \tag{3}$$

Here $F_{\lim}$ is the upper Froude number limit of steady subcritical one-dimensional flow, which is the smaller solution of

$$3\left[F_{\lim}^2\left(1-\frac{B}{w}\right)\right]^{\frac{1}{3}} - F_{\lim}^2\left(1-\frac{B}{w}\right) = 2\left(1-\frac{S_{\text{disp}}}{S_{\text{channel}}}\right) \tag{4}$$

(from **[7]**). S_{disp} is the displaced section area to the undisturbed waterline, S_{channel} is the channel area to the undisturbed waterline, and *B* is the local beam.

For steady subcritical flow, S_{disp} is simply the ship's section area *S*, while S_{channel} is the undisturbed area *wh* of the channel. Since the one-dimensional theory is a local theory, each point along the ship's length, having different values of *S* and *B*, will have its own limiting Froude numbers. The unsteady region is the envelope of these limiting Froude numbers, which is normally obtained using the values of *S* and *B* at the hull section of largest area.

A simple estimate of the bore characteristics can be found by using the limiting Froude number of steady subcritical flow, as described above, in equation (3). This method was introduced in **[5]**.

A more accurate and consistent solution is found by modifying the displaced area S_{disp} and channel area S_{channel} to allow for the new upstream water depth h_1 in the presence of the bore. If the ship is approximately wall-sided at midships, this gives

$$S_{\text{disp}} = S + (h_1 - h)B \tag{5}$$

$$S_{\text{channel}} = wh_1 \tag{6}$$

If the ship is approximately wall-sided at midships, *B* will be unchanged by the presence of the bore.

Upon substitution of equations (5,6), equations (1,2,3,4) constitute four simultaneous equations, for the four unknowns h_1, *W*, *V* and $F_{\lim}$, at each Froude number F_h. We can eliminate *W* and *V* from equations (1,2,3), to give

$$2\frac{h_1}{h}\left(F_h - \sqrt{\frac{h_1}{h}}F_{\lim}\right)^2 = \left(\frac{h_1}{h}-1\right)^2\left(\frac{h_1}{h}+1\right) \tag{7}$$

This can be rearranged to make $F_{\lim}$ the subject, i.e.

$$F_{\lim} = F_h \sqrt{\frac{h}{h_1}} - \frac{h}{h_1} \sqrt{\frac{1}{2}\left(\frac{h_1}{h} - 1\right)^2 \left(\frac{h_1}{h} + 1\right)} \qquad (8)$$

Substituting equation (8) for $F_{\lim}$ into equation (4) gives a single nonlinear equation which can be solved numerically for h_1. Thereafter, $F_{\lim}$, W and V can be found using equations (8,3,1) respectively.

2.2 Ship free to squat

In the case where the ship is free to squat, the displaced section area S_{disp} must be modified due to the ship's vertical displacement at each point. In terms of the longitudinal centre of floatation (LCF) upward heave z_{LCF}, and bow-up trim angle θ, the local heave z at any point x along the ship's length is

$$z = z_{\text{LCF}} + (x - x_{\text{LCF}}) \tan\theta \qquad (9)$$

The displaced area S_{disp} at each point along the ship's length is now decreased by the local heave, so that equation (5) is modified to

$$S_{\text{disp}} = S + (h_1 - h)B - zB \qquad (10)$$

for approximately wall-sided vessels.

The LCF heave and trim angle depend of course on the flow pattern past the whole ship, so that the bore properties cannot be solved accurately without computing the entire flow pattern past the ship. In addition, dynamic effects on heave and trim tend to be significant at supercritical speeds, so that hydrostatic methods are not sufficiently accurate for determining heave and trim in this case.

However, from free surface height calculations, it is expected that the maximum displaced section area when the ship is free to squat will not be significantly different from when it is vertically fixed. If this is the case, the bore properties should be similar to those produced by a vertically fixed ship.

3. One-dimensional free surface height theory

3.1 Ship vertically fixed in its rest position

We continue the notion that the flow behind the bore is analogous to a steady flow of undisturbed speed *U*-*W* and depth h_1 passing the ship, these values having now been found.

According to steady nonlinear one-dimensional theory **[8]**, the free surface height βh_1 above the still waterline (in this case having depth h_1) past the ship is the solution of the cubic equation

$$\frac{2}{F_h^2}\left(1-\frac{B}{w}\right)^2\beta^3+\left[\frac{4}{F_h^2}\left(1-\frac{S_{\text{disp}}}{S_{\text{channel}}}\right)\left(1-\frac{B}{w}\right)-\left(1-\frac{B}{w}\right)^2\right]\beta^2+$$
$$\left[\frac{2}{F_h^2}\left(1-\frac{S_{\text{disp}}}{S_{\text{channel}}}\right)^2-2\left(1-\frac{S_{\text{disp}}}{S_{\text{channel}}}\right)\left(1-\frac{B}{w}\right)\right]\beta-\left(1-\frac{S_{\text{disp}}}{S_{\text{channel}}}\right)^2+1=0 \qquad (11)$$

In this case, the Froude number F_h ahead of the ship's bow is replaced by F_{lim}, and S_{disp} and S_{channel} are modified by the presence of the bore as in equations (5,6).

Solution of equation (11), for each value of S and B along the length of the ship, gives the scaled free surface height β along the length of the ship.

The cubic (11) has between one and three real roots. The real root which is always present represents a backflow of negative cross-sectional area, which is impossible. The other two roots are both negative for $F_{\text{lim}}<1$, as is the case here. One of these represents slightly accelerated flow past the ship, with a slightly depressed free surface. For steady subcritical flow, this is the correct root, as it is statically stable (unlike the large free surface depression root) and the free surface must return to the undisturbed level behind the ship.

From the ship's bow back to the section of largest area, this solution with a slightly depressed free surface is the one we must choose. At the section of largest area, the two roots coincide, as this is how the limiting Froude number is defined. Any higher Froude number would result in no solution at this section.

The solution here differs from steady subcritical flow, in that because an elevated free surface is radiated ahead of the ship, a trough must be formed behind the ship. Therefore from the section of largest area to the stern, the free surface height must decrease, which requires that the solution for β must be the more negative of the two possible solutions. At the stern where S is small, the free surface height is significantly depressed.

For a cruiser stern, where S and B tend smoothly to zero at the stern, the theory then predicts a smooth flat trough behind the vessel. As such, the effect of the ship is to make the free surface act like a hydraulic jump in reverse: subcritical flow past the bow (relative to the ship) and supercritical flow past the stern.

For a transom stern (as is the case in our experiments) the sudden change in S and B at the stern cause a significant stern wave at about 45° to the vessel's track, so that the flow *behind* the ship cannot be modelled accurately using one-dimensional theory.

3.2 Ship free to squat

The more realistic case, where the ship is free to squat, is also more difficult due to the fact that the ship squat, free surface profile and bore are all interrelated. If z_{LCF} and θ are known or estimated, the displaced area S_{disp} is defined at each point along the ship's length by equations (9) and (10). Equations (4,8) can now be solved as

before for h_1 and $F_{\lim}$. Once these are found, the free surface height at any point along the ship's length is again the solution of equation (11), with S_{disp} modified as in equation (10).

It is possible to use this method by itself to calculate the sinkage, trim and free surface profile by iteration. Based on the free surface profile calculated for a particular sinkage and trim, a better estimate to the actual sinkage and trim can be obtained using hydrostatic balancing with the calculated free surface profile. The process can then be continued until convergence is reached.

As discussed earlier, however, hydrostatic balancing is not sufficient to describe sinkage and trim at these high Froude numbers, particularly for the beamy, flat-bottomed vessel used in our tests. As such, accurate estimates of the free surface profile can only be obtained using known or estimated values of z_{LCF} and θ.

4. Experimental procedure

Following on from the experimental program described in **[5]**, further shallow water experiments to observe ship bores were undertaken in the towing tank at the Australian Maritime College. The towing tank has length 60m and width w = 3.5m. A 1.6m AMECRC model #11 **[9]** was used. This is a transom stern round-bilge monohull, which has a parent hull the same as that of the High Speed Displacement Hull Form Series **[10]**. It has length L = 1.600m (between perpendiculars), waterline beam B = 0.400m, draft T = 0.100m, block coefficient $C_{\text{B}} = 0.50$ and midship section coefficient $C_{\text{M}} = 0.799$.

The depth was set to 0.125m for all tests, which was as small as possible without causing the model to ground. This allowed bores to be observed over the largest possible range of Froude numbers. This depth corresponds to a channel blockage coefficient (the ratio of the maximum ship section area to the channel cross-sectional area) of 0.073. This, as well as the beam/channel-width ratio B/w = 0.11, are the important non-dimensional parameters governing bore production (see equation (4)).

The model was attached to the carriage through two vertical posts, situated 0.385m ahead of and 0.415m aft of midships. Both attached to the model at approximately the vertical centre of resistance, with the forward post on a ball joint and the aft post on a sliding joint. Resistance was measured by a strain gauge at the bottom of the forward post. The posts themselves were counterbalanced, and could be either locked or free to slide vertically. Therefore the model was vertically fixed in its design waterline position for the initial round of tests, and allowed to sink and trim freely for subsequent tests. Hull drag was measured for all tests; heave and trim were measured for the unconstrained tests.

Two wave probes were positioned at equal distances from the channel wall and 2m apart along the channel. They were positioned near the end of the run to allow the bore to develop as completely as possible before measurement. The probes measured the free surface height as the model passed, and the time difference between wave front arrivals at each probe was used to determine the bore's average speed. Runs were made for gradually incremented supercritical speeds, through the complete

Froude number range from smooth soliton production, to bore production, to steady supercritical flow.

Fig. 2: Free-to-squat model at $F_h = 1.35$, showing carriage setup and bore radiating ahead of the model

5. Results

5.1 Bore properties

As noted in previous experiments **[5]**, all waves ahead of the ship were perfectly uniform across the tank in the soliton and bore-producing speed range. For both vertically fixed and free ship cases, solitons first began to break at $F_h \approx 1.1$. At higher Froude numbers, the solitons remained broken, with a fairly constant crest height of around 1.6 times the water depth. The troughs, however, increased in height with increasing Froude number; for $F_h > 1.3$ the waves resembled a raised flat shelf of water travelling ahead of the model, with a breaking bore front separating this elevated water from the undisturbed water ahead.

The transition to steady supercritical flow occurred experimentally at $F_h = 1.43$ for the free ship and at $F_h = 1.47$ for the fixed ship. According to equation (4), this transition is predicted to occur at $F_h = 1.44$ for the fixed ship in this particular case. Steady supercritical flow is possible at a smaller Froude number for the free ship, due to the rising of the vessel in the water and subsequently decreased maximum displaced cross-sectional area.

The uniformity of the free surface across the tank in the bore-producing speed range makes this flow ideal for the simple one-dimensional analysis described in Section 2. At lower Froude numbers, this theory is clearly unable to predict the height of individual peaks and troughs ahead of the model; it instead serves as an approximation to the mean free surface height ahead of the model. The theory has its best applicability at higher Froude numbers, when the flow ahead of the model resembles a pure bore.

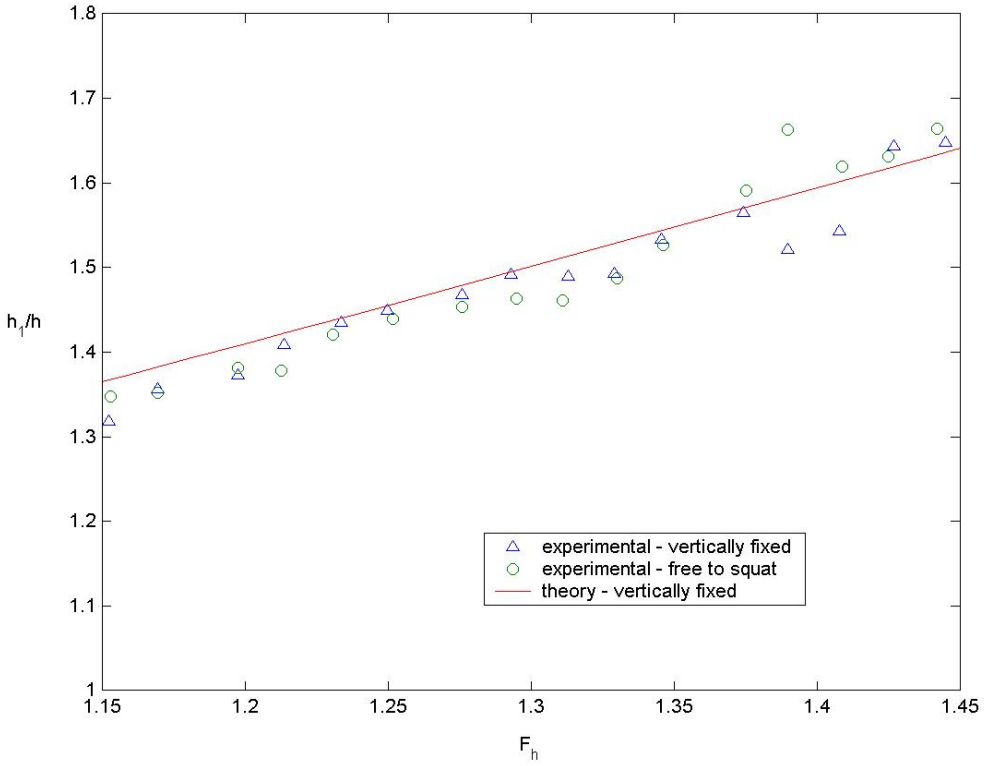

Fig. 3: Scaled bore height h_1 / h as a function of F_h; theory and experiment

Figure 3 shows the experimental mean free surface height h_1 above the channel floor, measured between the bow of the ship and the breaking bore front. This is scaled against the undisturbed water depth *h*. Results are shown for both the vertically fixed and free-to-squat model. In addition, the predicted bore height from one-dimensional theory (Section 2) is shown for a vertically fixed ship.

We see that there is very little difference between the bore produced by a vertically fixed or free-to-squat ship, despite the significant squat that occurs in this Froude number range. In addition, the fixed ship theory gives bore height results within 5% of the experimental values for both cases.

The present experimental results cannot be directly compared with the experimental results in **[5]**, since those experiments were conducted in a shallower depth. This resulted in a larger channel blockage coefficient and larger scaled bore height in the earlier experiments.

The modified theoretical results presented here show improved correlation with the experimental results, as the simplified theory presented in **[5]** slightly underestimated both the bore height and speed.

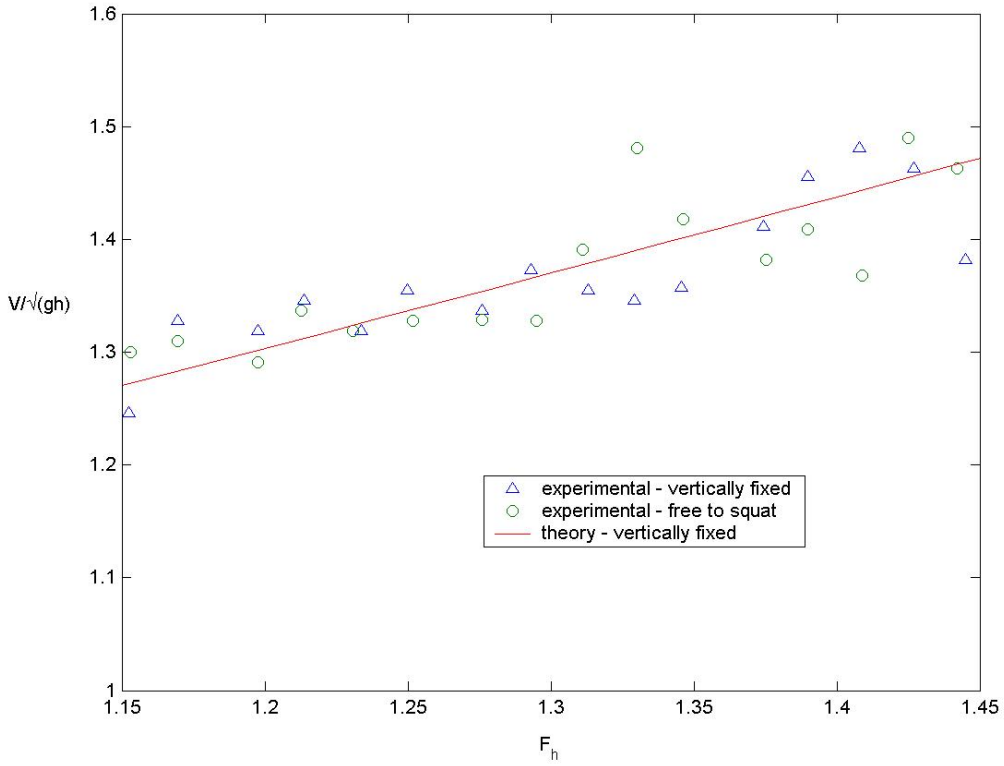

Fig. 4: Scaled bore speed $V/\sqrt{gh}$ as a function of F_h; theory and experiment

The bore speed for a vertically fixed or free-to-squat ship is shown in Figure 4, along with the predicted results from fixed-ship one-dimensional theory. Again, the results for each case are quite similar, and the new theory's predictions are within 6% of both the fixed ship and free-to-squat experimental observations. Given the approximate nature of this theory, these results suggest that one-dimensional fixed ship calculations should be adequate as a means of estimating the bore's speed and average height for a vertically fixed or free-to-squat vessel.

5.2 Heave, trim and drag on the hull

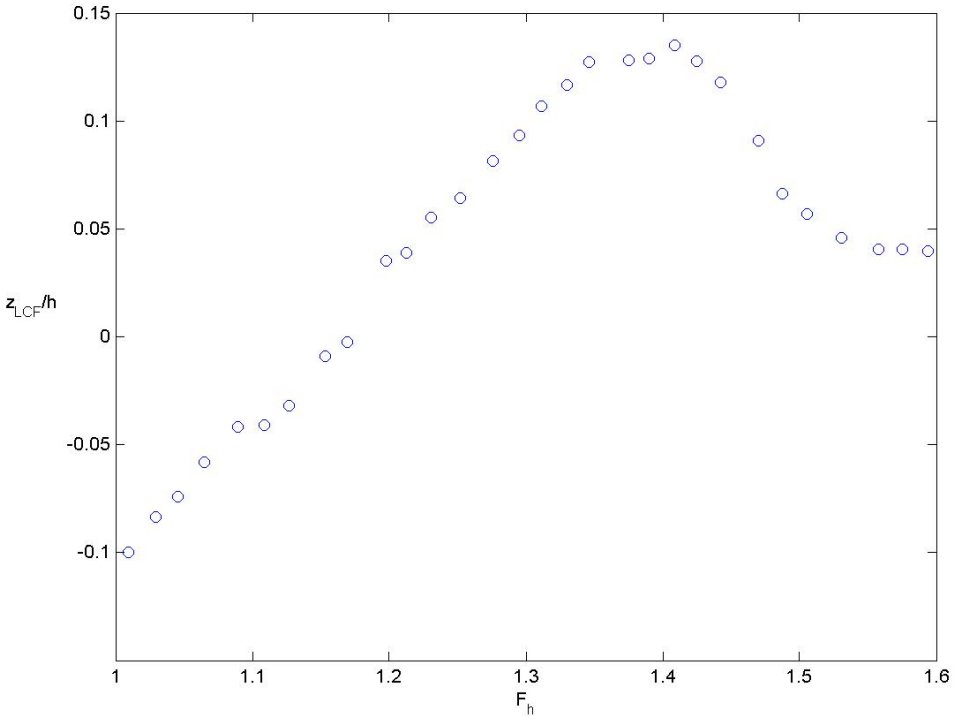

Fig. 5: Scaled LCF heave z_{LCF}/h as a function of F_h for free-to-squat ship

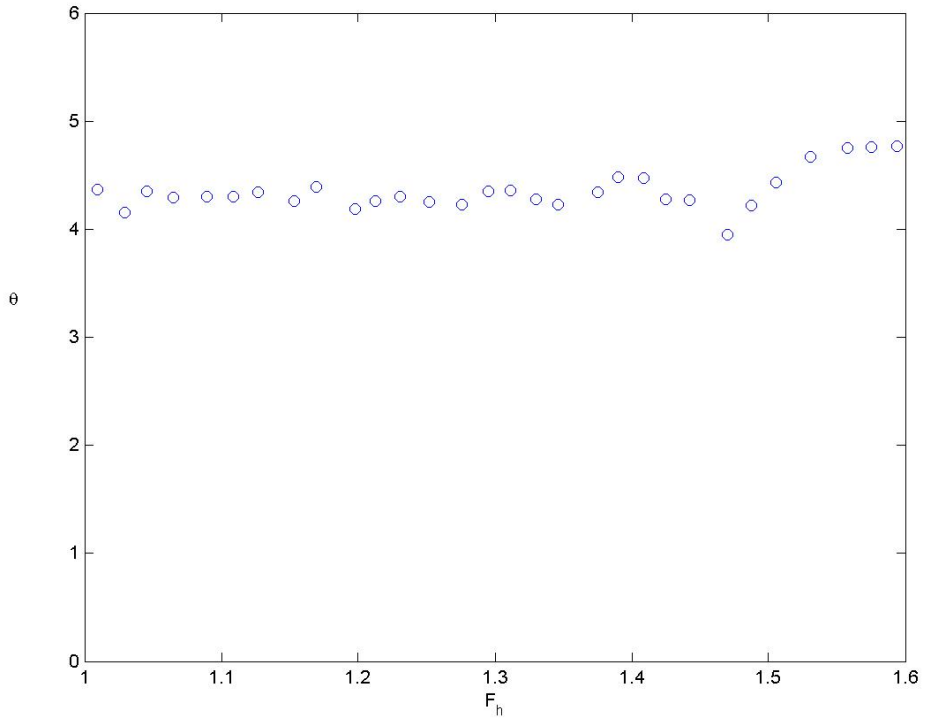

Fig. 6: Bow-up trim angle θ (in degrees) as a function of F_h for free-to-squat ship

The experimental mean heave (measured positive upwards) and trim (measured positive bow-up) of the free-to-squat ship are shown in Figures 5 and 6, respectively. For comparison, we have also included results outside the bore-producing Froude number range, i.e. including the smooth soliton region $F_h < 1.12$ and the steady supercritical region $F_h > 1.43$.

The main features of these graphs are a very large bow-up trim (around 4°) over the entire Froude number range, and a gradual rising of the vessel in the water up to the end of the bore-producing Froude number range.

The observed bow-up trim is roughly double that predicted based on hydrostatic assumptions, indicating that dynamic effects on squat are very significant at these Froude numbers for this type of vessel. This makes a complete prediction method for the free ship case seem unfeasible, due to the complex interrelation between the flow field and the vessel's squat.

Because the LCF of this vessel is well aft of midships (0.147m), the LCF heave is actually negative (downwards) at the lower Froude numbers, due to the large bow-up trim. The midship heave is positive over the entire range. However, the combination of heave and trim mean that the maximum displaced section area does not differ greatly between the fixed and free ship cases, explaining the negligible difference in bore properties witnessed in Figures 3 and 4.

Of interest is the behaviour of the vessel after transition to steady supercritical flow: a marked decrease in heave, accompanied by a temporary drop and subsequent increase in trim.

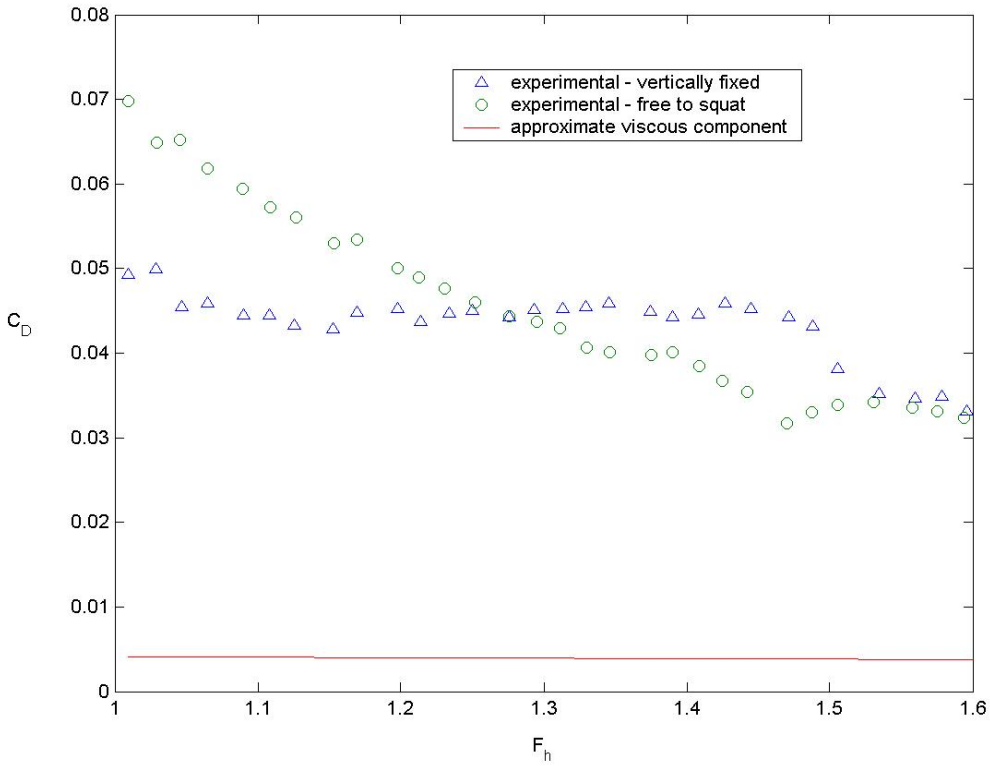

Fig. 7: Hull drag coefficient as a function of F_h

Figure 7 shows the hull drag coefficient (based on wetted area) $c_D = D/(\frac{1}{2}\rho U^2 S_{\text{wetted}})$, with the non-dimensional wetted area being $S_{\text{wetted}}/L^2 = 0.245$ for this hull. Experimental values are given for both the vertically fixed and free-to-squat vessel, and results are again given outside the bore-producing Froude number range for comparison. A rough approximation to the viscous component of resistance is given for both cases using the ITTC 1957 model correlation **[11]**

$$c_V \approx \frac{0.075}{(\log_{10} \text{Re}_L - 2)^2} \qquad (12)$$

Here Re_L is the Reynolds number based on ship length L and ship speed U. This formulation was used satisfactorily in resistance tests for this hull **[9]** and describes the Reynolds number dependent components of resistance, including both frictional resistance and form drag.

We see firstly that these drag coefficients are very large, with only around 10% of the total resistance coming from viscous effects. A simple verification of the large drag caused by the bore can be performed using the linear momentum equation (see e.g. **[12]**), assuming one-dimensional flow both ahead of and behind the ship. This is a crude approximation, since flow behind the ship is *not* one-dimensional due to the trailing waves from the vessel's stern. In terms of the free surface height h_2 and flow speed V_2 at the stern of the vessel (as calculated using the methods of Section 3.1), the linear momentum result gives the total drag D as

$$D = \rho w h_1 (U - W)^2 - \rho w h_2 V_2^2 + \frac{\rho g w}{2}\left(h_1^2 - h_2^2\right) \qquad (13)$$

Using calculated values of these quantities gives an estimated drag coefficient of around 0.03 – 0.05, in rough agreement with the measured values.

It is seen that the drag coefficient of the fixed ship remains approximately constant through the bore-producing Froude number range. The free ship's drag coefficient decreases with increasing Froude number, as it rises in the water and the maximum displaced section area decreases.

Both the fixed and free-to-squat vessels exhibit a marked decrease in drag coefficient when bore production ceases and steady supercritical flow starts. As discussed previously, this occurs at $F_h = 1.43$ for the free ship and at $F_h = 1.47$ for the fixed ship.

5.3 Free surface height past the ship

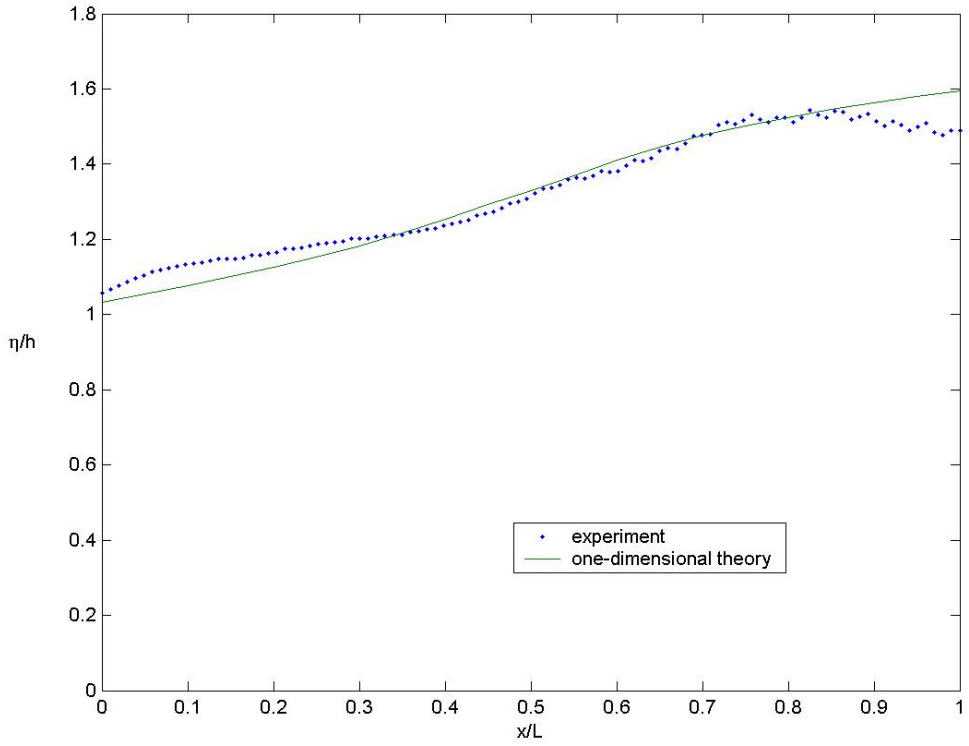

Fig. 8: Scaled free surface height η / h past vertically fixed ship at $F_h = 1.40$; theory and experiment

Figure 8 shows the free surface profile past the ship vertically fixed in its rest position at $F_h = 1.40$. The free surface height η above the sea floor is scaled against the undisturbed water depth *h*; this is plotted as a function of distance along the ship *x*, scaled against the ship length *L*. The stern of the ship is at $x / L = 0$, and the bow is at $x / L = 1$.

The experimental free surface profile $\eta(x)$ is assumed steady over a short time period, since we are considering high Froude numbers where the bore height and

speed, as well as free surface past the ship, are approximately steady. $\eta(x)$ can therefore be obtained from the wave probe data $\eta_{\text{probe}}(t)$, which is measured at a fixed point as a function of time. Specifically, if the time that the ship's stern passes the wave probe is t_0, the transformation

$$x = -U(t - t_0)$$

gives the points *x* along the ship's hull that correspond to the wave probe's measurements at time *t*. Therefore $\eta(x)$ is given by $\eta_{\text{probe}}(t)$ at the time values $t = t_0 - \frac{x}{U}$.

The wave probes used to collect free surface height data were both positioned 1.5m from the centreline of the model. Visual observations suggest that ahead of the ship's stern, the flow is very nearly uniform across the tank, so that these results should also represent the flow across the whole tank. However, in the absence of other wave probe data in the transverse direction, the exact deviation from constant free surface height across the tank cannot be quantified.

The results of one-dimensional theory are also shown in Figure 8; in this case η is found by solving equation (11) for β at each point along the hull, whereupon $\eta = (1+\beta)h_1$ at each point.

Another example is shown in Figure 9, where we have plotted the same free surface height but at the higher Froude number $F_h = 1.44$.

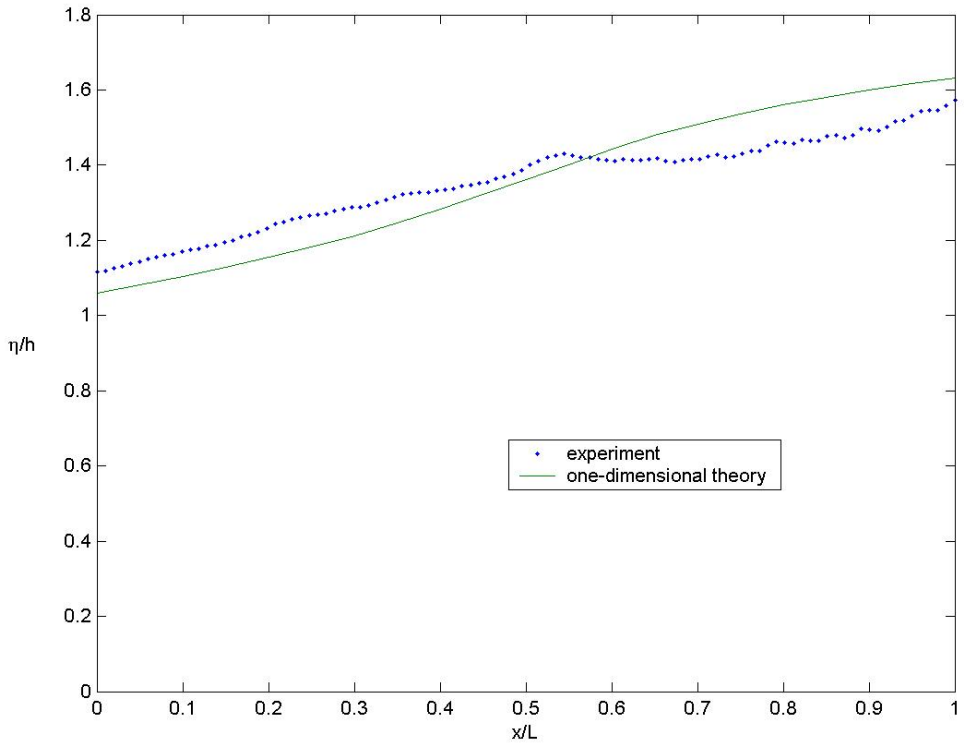

Fig. 9: Scaled free surface height η / h past vertically fixed ship at $F_h = 1.44$; theory and experiment

As stated previously, this simple one-dimensional theory is unable to predict the superposed one-dimensional waves, instead being an approximation to the overall free surface height. However, we see that one-dimensional theory provides a good approximation to the free surface height along the length of the vessel. At the higher Froude numbers, where the superposed waves are small, the theory provides a closer estimate to the entire free surface profile.

We see that in both these cases the free surface is above the still waterline along the entire length of the vessel. Of course, the presence of an elevated and advancing bore ahead of the ship means that a trough must be formed behind the ship, from mass conservation. However, due to the large beam at the ship's stern in this case, this trough is not formed until behind the ship's stern. The trough itself is not one-dimensional in nature due to the trailing waves coming from the ship's stern, so the present theory is only useful from the stern of the vessel forward.

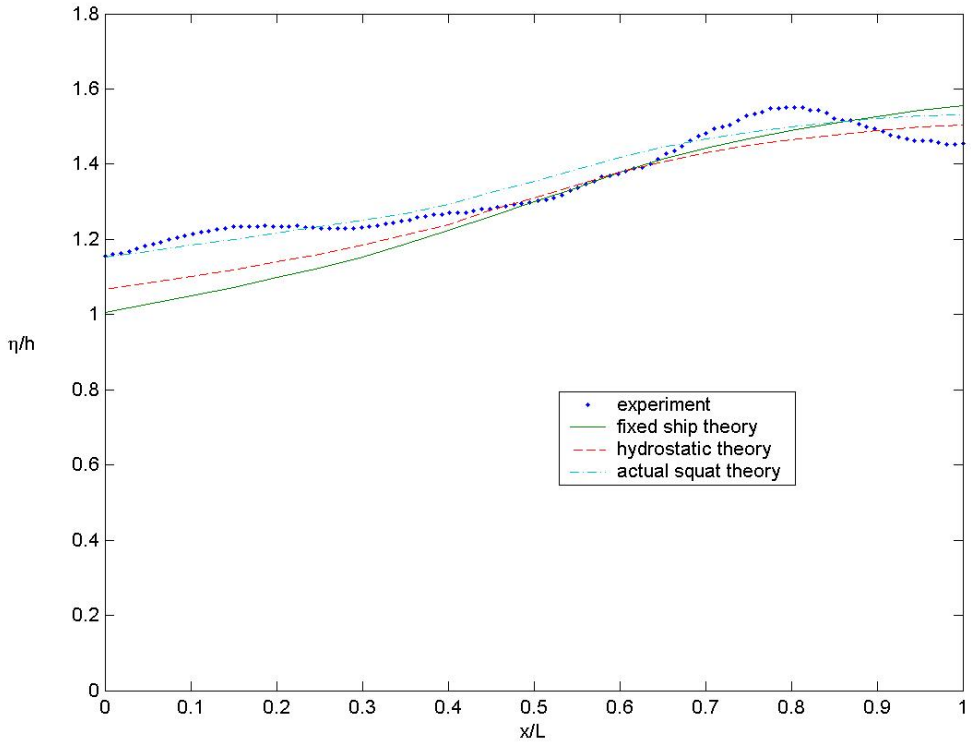

Fig. 10: Scaled free surface height η / h past free-to-squat ship at $F_h = 1.36$; theory and experiment

Figure 10 shows an example free surface profile (at $F_h = 1.36$) past the ship when it is free to squat. Experimental results are shown, as well as the results of three separate theories: basic fixed ship theory (as described in Section 3.1); free ship theory (Section 3.2) based on hydrostatic balancing; and actual squat theory. Actual squat theory uses modified values for S_{disp} in equation (11), based on actual measured sinkage and trim.

We see that fixed ship theory is relatively inaccurate, due to the large trim angle of the free ship and its effect on the displaced section areas. The method using hydrostatic

balancing is better, but because it only predicts a bow-up trim of around 2° (compared to the measured value of around 4°) it is not as good as the method based on actual sinkage and trim. This last method provides a good estimate to the mean free surface height past the ship, but cannot be calculated without knowing the sinkage and trim.

Conclusions

The bore produced by a ship travelling in a shallow, narrow channel at slightly faster than the critical speed has been studied. An improved method for estimating the bore's height and speed has been put forward, and found to be in good agreement with experimental results for both a vertically-fixed and free-to-squat ship. It was found that the more complicated free-to-squat theory put forward here was unnecessary as a means of predicting the bore's height and speed; these were very similar to the case of a fixed ship, whose analysis is easier. In addition, the difficulty in relating sinkage and trim to flow properties at high Froude numbers makes this theory less useful.

The actual sinkage and trim of a free-to-squat ship were studied experimentally for the particular hull form. It was found that the bow-up trim angle was a very large 4° over the whole bore-producing Froude number range. The LCF rose in the water with increasing Froude number, up to the transition to steady supercritical flow.

Hull drag was measured experimentally. It was found that the drag in the bore-producing Froude number range is very high, with around 90% of the drag being caused by wave drag for this particular hull. A simple force-momentum analysis of the radiated bore verifies this large drag.

Nonlinear one-dimensional theory has been extended to predict the free surface height along the entire length of the vessel. This has been shown to be in good agreement with experiment for a vertically-fixed ship, and fair agreement for a free-to-squat ship. In the latter case, a better estimate may be found using hydrostatic balancing in the analysis to calculate sinkage and trim, and a still better estimate by using the actual measured sinkage and trim.

Acknowledgement

The authors wish to acknowledge the support of the Australian Maritime College in allowing the experimental testing to be conducted.

References

1. **Thews, J.G. and Landweber, L.** The influence of shallow water on the resistance of a cruiser model. US Experimental Model Basin, Navy Yard, Washington DC, 1935, Rep. 408.
2. **Huang, D.B., Sibul, O.J., Webster, W.C., Wehausen, J.V., Wu, D.M. and Wu, T.Y.** Ships moving in the transcritical range. *Proc. Conference on Behaviour of Ships in Restricted Waters, Varna,* 1982, Vol II, 26/1-10.
3. **Ertekin, R.C., Webster, W.C. and Wehausen, J.V.** Ship-generated solitons. *15th Symp. Naval Hydrodynamics,* 1985, 347-361. Washington DC. National Academic Press.
4. **Lee, S.J., Yates, G.T. and Wu, T.Y.** Experiments and analyses of upstream-advancing solitary waves generated by moving disturbances. *J. Fluid Mech.* 1989, **199**, 569-593.

5. **Gourlay, T.P.** The supercritical bore produced by a high-speed ship in a channel. *J. Fluid Mech.* 2001, **434**, 399-409.
6. **Stoker, J.J.** Water Waves. 1957, Interscience, p.321.
7. **Tuck, E.O.** One-dimensional flows as slender-body problems, with applications to ships moving in channels. *Proc. Workshop on Slender-Body Theory, Ann Arbor, Michigan, University of Michigan Rep. NAME* 1974, Vol. 164, 27-35.
8. **Gourlay, T.P.** The effect of squat on steady nonlinear hydraulic flow past a ship in a channel. *Schiffstechnik* 1999, **46**(4), 217-222.
9. **Bojovic, P.** Resistance of AME CRC Systematic Series of high speed displacement hull forms. *Proc. 4th Symp. On High Speed Marine Vehicles, Naples, Italy*, 1997. ATENA / CETENA / Dipartimento do Ingegneria Navale, Universita di Napoli Frederico II.
10. **Robson, B.L.** Systematic Series of High Speed Displacement hull forms for naval combatants. *Trans. R. Inst. Nav. Archit.* 1988, **130**, 241-252.
11. **International Towing Tank Conference.** *Proc 8th ITTC, Madrid, Spain,* 1957, published by Canal de Experiencias Hidrodinamicas, El Prado, Madrid.
12. **White, F.M.** Fluid Mechanics, 4th Ed. 1999, McGraw-Hill, p.146.